Dynamic spin susceptibility of semimagnetic semiconductors

Marek Cieplak
Institute of Theoretical Physics, Warsaw University, 00-681 Warsaw, Poland

Marta Z. Cieplak
Institute of Physics, Polish Academy of Sciences, 02-668 Warsaw, Poland

J. Łusakowski
Institute of Experimental Physics, Warsaw University, 00-681 Warsaw, Poland
(Received 22 September 1986)

Semimagnetic semiconductors with frustration are modeled by Ising spins populating a fcc lattice and coupled by nearest-neighbor antiferromagnetic interactions. The system is endowed with Glauber dynamics. At small concentrations the system is a collection of various n-spin clusters. We obtain statistical weights of these clusters at different compositions. We calculate equilibrium and dynamic susceptibilities. Clusters containing up to seven spins were included. The dynamics of each cluster are solved exactly. Each cluster contributes as many long relaxation times as it has nontrivial ordinary and extended energy minima. The barriers against inversion of the clusters take only three values: 0, $2|J|$, and $4|J|$. At low temperatures this results, via the Arrhenius law, in a three-peaked distribution of the relaxation times on a logarithmic scale. Such a structured spectrum yields a χ' with three plateaus and a χ'' with three maxima when plotted against $\log\omega$.

I. INTRODUCTION

The most noticeable features of spin-glass dynamics are the slow decay of fluctuations and the existence of a broad spectrum of relaxation times as shown, e.g., by Chamberlin *et al.*,[1] Mezei and Murani,[2] and Lundgren *et al.*[3-5] A sensible way to try to understand these phenomena would seem to be the study of the dynamics of small clusters, in order to examine effects of the incipient multiminima physics. This approach has been taken by Kinzel,[6] Banavar *et al.*,[7] Reger and Binder,[8] and Cieplak and Łusakowski.[9] The first and third of these papers considered ensembles of rings with spins. On the other hand, the other two papers dealt with a single six-spin cluster characterized by a coordination number of 4. All of these papers discussed Ising spins with single-spin Glauber[10] dynamics. This yields a linear equation of motions for $\langle S_i \rangle$ in the case of rings and nonlinear ones in the other cases.

The focus of Banavar *et al.* and Cieplak and Łusakowski (henceforth referred to as BCM and CŁ) was on finding links between properties of the local energy minima and the resulting spectra of relaxation times. These in turn have been used to explain the frequency-dependent susceptibility. The findings, in the absence of a static field, can be summarized as follows.

The decay of a remanent magnetization is governed by a sum of 2^n-1 exponential terms, where n denotes the number of spins in a cluster. Most of the corresponding relaxation times are short—of the order of the microscopic Glauber time τ_0. There are some relaxation processes, however, which become infinitely long in the limit of $T\rightarrow 0$. The number of such diverging relaxation times is equal to the number of nontrivial local energy minima which are stable against single-spin reversals. (By nontrivial, we mean that we do not consider a state obtained by reversing all of the spins as a different energy minimum.) The diverging relaxation times follow an Arrhenius law,

$$\tau_\nu=\tau_0' e^{\varepsilon/k_B T}, \tag{1}$$

where ε is the energy barrier against inverting the minimum upside down. The prefactor τ_0' is of the order of τ_0. (Strictly speaking, the reversals of the true ground states have been studied in CŁ, but the same property is expected for excited minima as well.) Depending on T and on the exchange couplings, the diverging relaxation times can either be close to each other, on a logarithmic scale, or be noticeably separated. In the latter case the real part of frequency-dependent susceptibility, $\chi'(T,\omega)$, reveals a sequence of plateaus as a function of $\log\omega$, whereas the imaginary part, $\chi''(T,\omega)$, displays maxima.

Experimental results for χ'' are usually plotted versus ω, and not versus $\log\omega$. However, the experiments of Lundgren *et al.*[3-5] on metallic spin glasses tend to indicate the absence of maxima in χ''. This may serve as a partial justification of the phenomenological model proposed by Lundgren *et al.*[3] in which one postulates that the relevant relaxation times are distributed uniformly on a logarithmic scale.

The relaxation times are related to barriers against reversals of the minima. One expects, therefore, that the spectrum of these times will be uniform on a log scale provided the exchange couplings come from a set which is effectively continuous, e.g., Gaussian numbers. If the couplings are two valued as in the case of $Eu_xSr_{1-x}S$ (see, e.g., Eiselt *et al.*[11]), then the possibility exists for a structured distribution of the relaxation times.

A similar situation, but in an even more pure form, can

be found in the so-called semimagnetic semiconductors reviewed by Mycielski[12] and Galazka.[13] Examples of these are $Cd_{1-x}Mn_xTe$ studied by Galazka *et al.*[14] and $Hg_{1-x}Mn_xTe$ studied by Nagata *et al.*[15] In both these compounds the $S=\frac{5}{2}$ manganese ions occupy sites of a fcc lattice and the neighboring ions are coupled by an antiferromagnetic interaction J of the order of -13.8 ± 0.3 K in the case of $Cd_{1-x}Mn_xTe$ and -14.3 ± 0.5 K in the other semiconductor.[16] It is possible to include antiferromagnetic next-nearest-neighbor couplings in any theoretical account of the magnetic properties of the two systems. These, however, do not alter the essentials of the physics involved: the peculiarities of the fcc geometry can make the systems behave like spin glasses even with only nearest-neighbor antiferromagnetic couplings. A Monte Carlo study which demonstrates this, at least for Ising spins, is that of Grest and Gabl.[17]

With the next-nearest-neighbor couplings excluded a spin-glass behavior is expected above the percolation threshold, i.e., for $x>x_c=0.195$ (at sufficiently large x an antiferromagnetic order sets in). Below the threshold the spins form finite clusters and nothing but a paramagnetic phase is possible.

Recently, however, evidence for spin-glass behavior significantly below x_c, e.g., at $x=0.01$ and $T<1$ K, has been presented. This suggests the influence of longer-ranged forces. In the case of $Hg_{1-x}Mn_xTe$ the evidence is due to Brandt *et al.*[18] and in the case of $Cd_{1-x}Mn_xTe$ and $Cd_{1-x}Mn_xSe$ to Novak *et al.*[19] Similar conclusions have been reached for $Zn_{1-x}Mn_xSe$ and $Zn_{1-x}Mn_xTe$ by Twardowski *et al.*[20] In the latter paper an ac susceptibility ($\omega>100$ Hz) is measured to get a freezing temperature T_f. Novak *et al.* made measurements of the magnetization at $H=1$ Oe and attempted to locate an equilibrium T_f by waiting for 2 h or so after any change in T. At the lowest temperatures studied by the two groups, of the order of 0.01 K, both experiments seem to occur too fast for the study of equilibrium. As we shall see, the highest barriers ε of independent clusters involved here should be of the order of $4|J|$. In translating the Glauber dynamics into real life the time τ_0' is typically assumed to be about 10^{-12} sec. Thus Eq. (1) yields the longest relaxation time to be roughly equal to $10^{-12}e^{56/T}$ sec. For $T=1$ and 2 K this gives τ of the order of 10^{12} and 1.4 sec, respectively. Any interactions between clusters should extend relaxation times even further. Above $T=2$ K and much below the threshold x_c the two experiments are probably on the safe side. Above the threshold, at $x=0.4$, Ferré *et at.*[21] report processes lasting for 100 sec in $Cd_{1-x}Mn_xTe$.

The nature of the longer-ranged forces is a matter of a dispute. Novak *et al.* explain their data in terms of dipole-dipole interactions. In the two known cases in which a purely dipolar ordering is found to exist the ordering temperatures are equal to 0.136 and 0.02 K (after Ref. 22). Thus at several degrees Kelvin these interactions are not expected to matter. Twardowski *et al.*, on the other hand, invoke unknown $R^{-6.8}$ forces between spins.

Either way, it seems proper to assume that at not too low temperatures, say $T>1$ K, and not too large concentrations, say $x<0.08$, an independent-cluster picture should work well. Studying the dynamic susceptibility of such clusters is an object of the present studies. The major simplification adopted here consists of replacing the manganese spins by the Ising ones which take values of $+$ and -1. It is hoped that the essential physics is still retained in this way. Note that there can probably be no spin glass with purely Heisenberg-like spins in three dimensions (see Refs. 23–26). In the case of $Cd_{1-x}Mn_xTe$, the Isinglike anisotropies could perhaps originate in local elastic stresses. Nevertheless, the role of the transverse-spin interactions as well as the quantum effects in the spin relaxation are hard problems to be still elucidated.

In the research we report on here we have generated all of clusters that are relevant at small concentrations. We then studied their magnetic properties and found a generalized rule that associates the number of diverging relaxation times to energy minima. At low temperatures the distribution of the logarithms of these times is not uniform. Instead, it has been found to be confined to three different regions. This is because there are only three possible energy barriers ε in these clusters: 0, $2|J|$, and $4|J|$. This structure of the spectrum results, at low temperatures, in a three-peaked χ'' and a three-plateaued χ' when plotted against $\log\omega$. It remains as an interesting question whether the peaks could be seen experimentally before the long-ranged interactions begin to alter relaxation patterns. And the way in which these forces affect the dynamics is still another interesting question to ponder.

II. GEOMETRY OF CLUSTERS

The statistics of the relevant clusters has been obtained numerically. We considered a fcc lattice consisting of four cubic sublattices, $12\times12\times12$ sites each. The periodic boundary conditions were used. The sites were populated with spins with a probability x. For each x, $C=40$ samples have been taken into account. We have considered x between 0.01 and 0.18 and identified two different three-spin clusters, six clusters with $n=4$, 15 with $n=5$, 40 with $n=6$, 72 with $n=7$, 116 with $n=8$, and 134 with $n=9$. Clearly a proper account of the $n=8$ and 9 clusters needs a significant improvement in the sample statistics. In calculations of the susceptibility we considered clusters consisting of up to seven spins which restricts the physical relevance of our studies to concentrations not exceeding about 0.08. We estimate that at this concentration the contribution of clusters with $n>8$ to the total number of available clusters is about 10%.

Figures 1–3 show all of our $n\leq6$ clusters. We have divided them into three different types for reasons which will become clear later. The pictures of the clusters are merely schematic since the only geometrical features that matter in calculations of the susceptibility are local coordination numbers and the pattern of the links. We have tabulated the statistical weights with which particular clusters appear at a given concentration. These weights were calculated according to the following formula:

$$P(\lambda,n)=\frac{n}{C}\sum_c\frac{m_\lambda(c)}{N_c}\ , \tag{2}$$

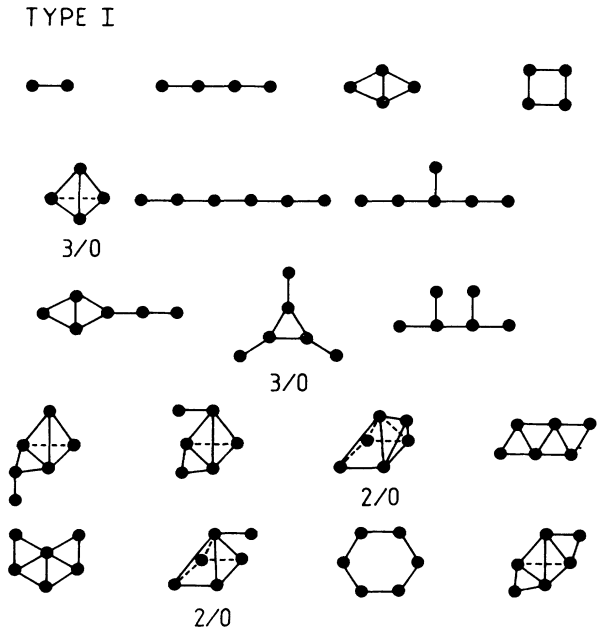

FIG. 1. Clusters of type I which consist of $n \leq 6$ spins. These clusters have the static susceptibility approaching 0 in the limit of $T \rightarrow 0$. The significance of the numbers shown is explained in the text.

where c enumerates samples, N_c denotes the number of occupied sites, and $m_\lambda(c)$ counts clusters of kind λ. In other words, $P(\lambda,n)$ gives a probability that a lattice site, if taken, belongs to an n-spin cluster of shape λ. The weights $P(\lambda,n)$ are available upon request. We just mention here that for a given n most probable are those clusters which are "linear" or are simple "one-leg" or one-triangle additions to the linear objects. Compact and highly coordinates clusters are less probable. There is no truly overwhelming type of cluster though.

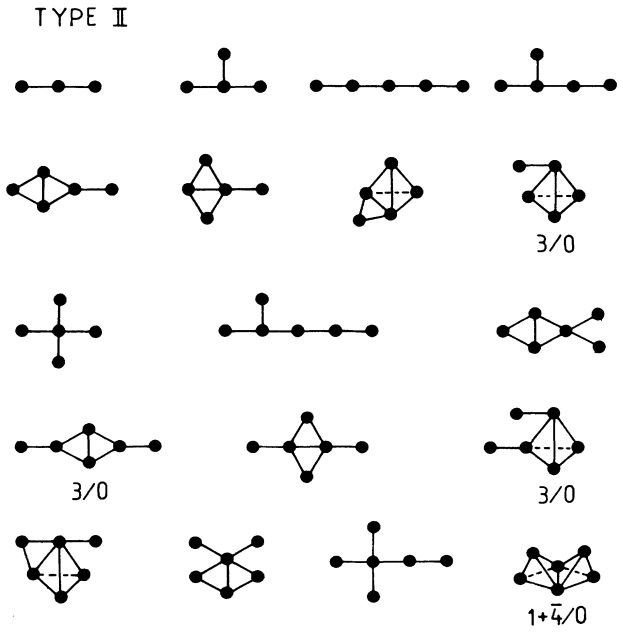

FIG. 2. Clusters of type II which consist of $n \leq 6$ spins. These clusters have a diverging static susceptibility and have ground states which are not extended.

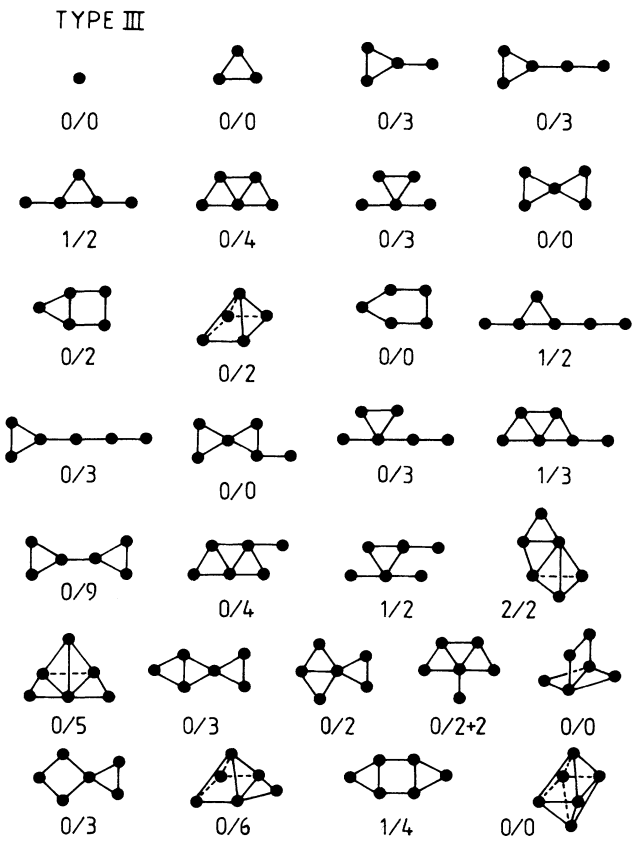

FIG. 3. Clusters of type III which consist of $n \leq 6$ spins. These clusters have a diverging static susceptibility and have ground states which are either extended or allow for their reversals without any energy cost.

Figure 4 shows a probability P_n for a cluster to consist of n spins. P_n is derived by adding weights of all the n-spin clusters. We see that no matter what $x < x_c$, single-spin clusters are invariably the most probable clusters around. In general, P_n monotonically decreases with n. The authors of Refs. 14 and 15 make fits to experimental susceptibility and specific heat at $x = 0.027$ and 0.06 based on up to $n = 3$ clusters. They conclude that somehow single spins are less abundant, by 30% or so, than a perfectly random distribution would yield. This propensity for correlated clustering can be explained more simply by invoking a necessity to include higher n clusters as Fig. 4 suggests. Our calculations show also that the $n \leq 3$ clusters exhaust 84.70% of possibilities for an occupied site at $x = 0.06$. Novak *et al.*[19] argue similarly that the spin distribution is, in fact, random, but single spins, or for that matter any clusters, disappear as such due to couplings via the dipolar interactions.

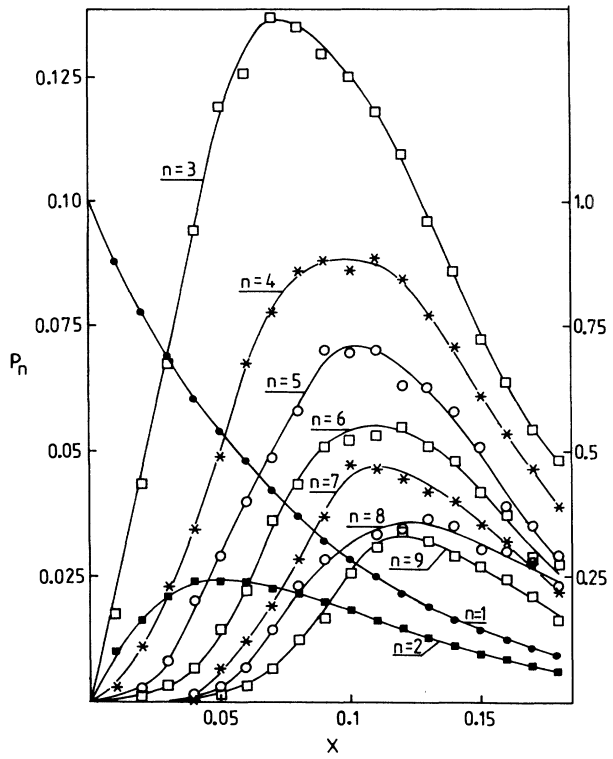

FIG. 4. Probability P_n for a cluster to consist of n spins, $n=1-9$, as a function of the concentration x. The scale for $n=1$ and 2 is shown on the right. The scale for other values of n is shown on the left.

Note that P_n has a maximum when plotted against x. The maximum shifts towards higher x upon increasing n. The value of $x=0.08$ adopted in most of our calculations of the susceptibility is halfway between the maxima for $n=3$ and 4. The $n \geq 8$ clusters clearly make a contribution then. Our aim, however, is not strict accuracy, but rather to show the role of the clusters with $n \geq 4$.

III. ENERGY MINIMA

For any of the n-spin clusters we can scan through their 2^n states and observe energy changes upon reversing individual spins. It is convenient to distinguish between the following categories of states:

(a) ordinary energy minima, i.e., states which are stable against single-spin reversals;

(b) extended minima, i.e., states in which it costs no energy to turn some of the spins but a positive energy to move the remaining ones; the system, so to speak, can float freely within several of such states; their number will be referred to as an extension of the minimum;

(c) totally frustrated states, i.e., those which are extended so much that their inverted image contributes to the extension of the state.

The totally frustrated states appear, e.g., on the last cluster of Fig. 3 studied in BCM and CL. For $J_{ij}=J<0$ it costs no energy to invert the ground-state spin configuration on this cluster and this yields merely a finite relaxation time. By extended minima we do not mean the totally frustrated states.

We now classify clusters according to the properties of their extended and ordinary energy minima. It is convenient to describe an energetic structure of a cluster by a symbol l/m where l denotes a number of nontrivial ordinary energy minima and m specifies extension of a nontrivial extended minimum. These symbols are used in Figs. 1–3. If no symbol is displayed the cluster is meant to have just a single energy minimum, i.e., it yields a 1/0 structure. An overbar indicates a minimum which is not a ground state. Thus $1+\bar{4}/0$ denotes a system in which the ground state is not degenerate (other than the trivial degeneracy of a mirror reversal) and in which there are four degenerate excited minima. There are no extended states here. In particular, this means that there is no cost-free path between the four minima. The symbol 0/3 means that there is one extended minimum whose extension is 3. All extended minima shown in the figures correspond to ground states. Thus $0/2+2$ means that the ground state consists of two groups of doubly extended states (plus the inverted images). All of these states are identical in energy. Otherwise an overbar would distinguish the states which are excited. The symbol 1/4 indicates that the ordinary and a fourfold extended minimum coexist at the same energy. An example of a 1/4 cluster is shown in Fig. 5 together with its nontrivial ordinary and extended energy minima. The classification of the clusters is as follows.

(a) Type I: clusters in which the ground state or states are ordinary energy minima and in which an overall magnetization vanishes. This can happen only for even n since only then it is possible to have as many spins up as down.

(b) Type II: same as above except for a demand that the ground-state magnetization is nonzero.

(c) Type III: at least one of the ground states is extended.

The physical relevance of this classification will be explained shortly. Let us now characterize statistical weights of the particular types. At $x=0.04$ there are 26.25% of taken sites which belong to $n \leq 6$ clusters of type I, 9.55% of sites with $n \leq 6$ clusters of type II, and

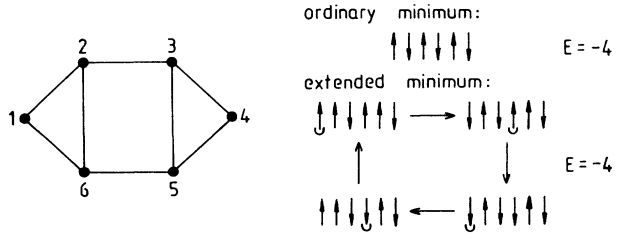

FIG. 5. The 1/4 six-spin cluster of type III. It is the next to the last cluster of Fig. 4. The "bowls" indicate cost-free single-spin reversals. A barrier against complete reversal of each of the five states shown is equal to $2|J|$.

64.00% of type III. At $x=0.08$ the corresponding numbers read 28.75%, 16.04%, and 45.90%, respectively. These numbers add up to 90.70% and the remaining clusters consist of seven and more spins. The third type clearly dominates at the expense of the second type.

The bulk of type-I clusters are the two-spin ones. At $x=0.04$ and 0.08 they make 23.82% and 21.59% of all the occupied sites, respectively. In the second type the linear three-spin clusters predominate (7.74% and 11.10% correspondingly). Finally, most of the type-III clusters are single spins (60.40% and 36.84%).

IV. STATIC SUSCEPTIBILITY

The thermal average of S_i, $\langle S_i \rangle$, is equal to zero for each cluster. It follows that the static susceptibility of a cluster of shape χ_λ is equal to

$$\chi_\lambda = \frac{1}{k_B T}\left\langle \left[\sum_{i=1}^{n} S_i \right]^2 \right\rangle . \tag{3}$$

In order to determine the susceptibility χ per lattice site we multiply χ_λ by $P(\lambda,n)$. This is then multiplied by x; that is, by the probability to occupy a site. Finally, a summation over all of the $n \leq 7$ clusters is performed.

Let us first fix T and investigate the x dependence of χ. Figure 6 shows χ at $T=0.2$ (in units of $|J|/k_B$) together with contributions to χ from clusters of a given n. The $n=2$ cluster yields practically no contribution at such a low T. The most important clusters here are the $n=1$, 3, and then the $n=5$ clusters. At $x=0.06$ (see Ref. 15) the clusters with $n \leq 3$ make about 82% of the net susceptibility. At $T=0.4$ they count about the same. The net susceptibility bends at $x \approx 0.11$. Including larger clusters will move the maximum more to the right. It is interesting to note that the experimental susceptibility displays a similar maximum in the vicinity of $x=0.15$ or so.[15]

Figure 7 shows $1/\chi$ versus T at various concentrations. The slope of $1/\chi$ gives an inverse of the Curie constant. The Curie constant grows with x in the way that mimics the experimental findings.[14–16] This also testifies to a relevance of our model to describe semimagnetic semiconductors.

We now examine the T dependence of χ in a little more detail. A typical χ-versus-T plot is shown in Fig. 8. This time we single out contributions from the three major types of clusters as defined in the preceding section. Clusters of type I yield a susceptibility that vanishes at $T=0$ exponentially. The other two types diverge as $1/T$ and overall we get a divergence.

The described behavior of the susceptibility is very easy to understand. At low temperatures the dominant contribution comes from ground states of the clusters. If these states, as in the type-I clusters, are not magnetized, then the corresponding χ must disappear in the low-T limit. Clearly, the clusters of type II must yield a finite $\langle (S_i)^2 \rangle$

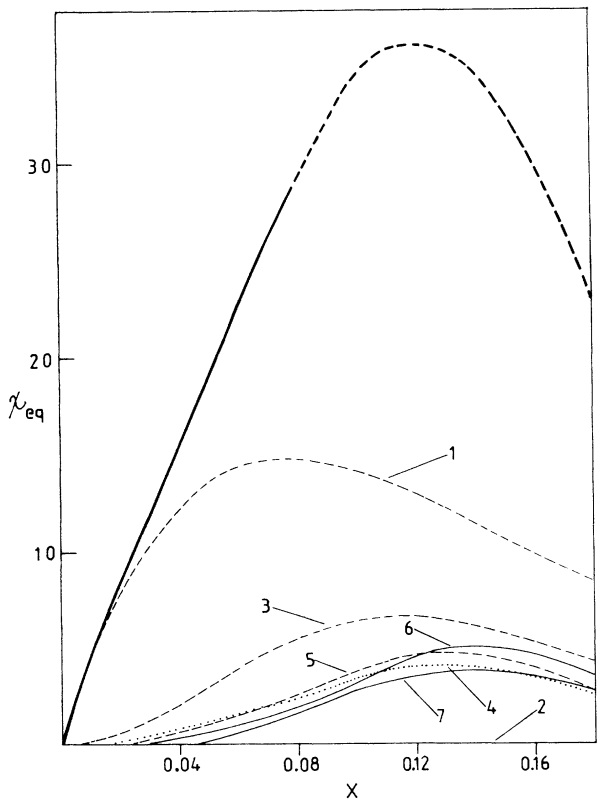

FIG. 6. Static susceptibility at $T=0.2$ vs x. The bold solid line shows the net result, as does its dashed continuation to x exceeding 0.08. The thin solid lines show contributions from clusters of an indicated number of spins.

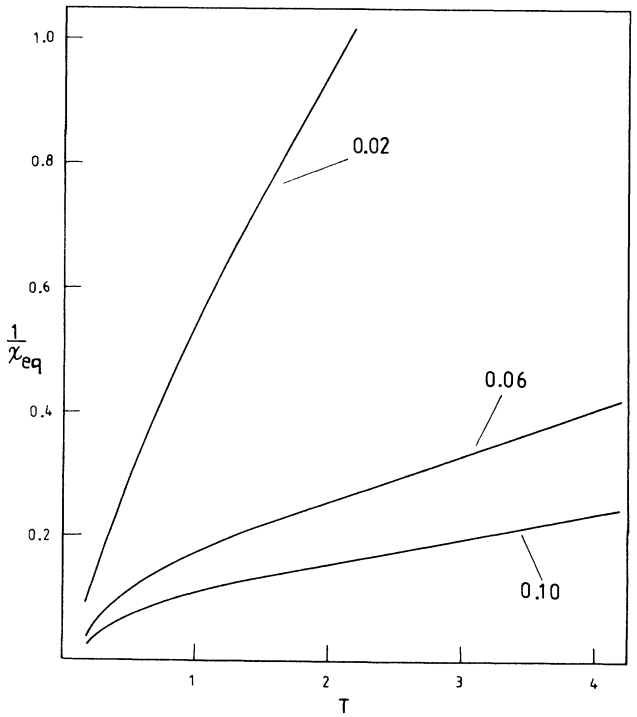

FIG. 7. Inverse of the static susceptibility vs T for $x=0.02$ and higher in increments of 0.04

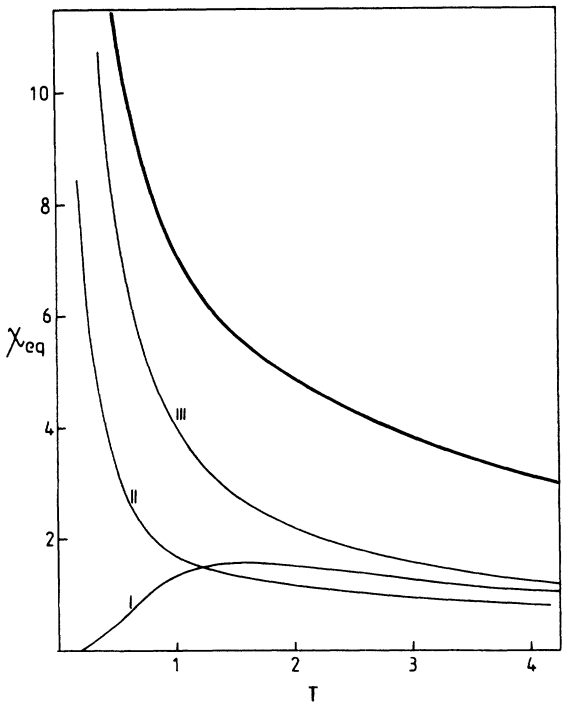

FIG. 8. Static susceptibility at $x=0.08$ vs T. The bold solid line shows the net result. The thin solid lines indicate contributions from the three types of clusters.

and thus a divergent χ. In the case of the third type of cluster the ground states are either (totally or partially) extended or totally frustrated. The "flow" across these states must necessarily go through states which are magnetized and thus yield a finite $\langle (S_i)^2 \rangle$. We shall see that the type-II and type-III clusters display an entirely different dynamic behavior though.

V. SPECTRUM OF RELAXATION TIMES

Suppose the system is kept in a magnetic field which is then turned off. With what relaxation times will the magnetization disappear? According to Glauber the anwser to this question reduces to solving the equations of motion as

$$\left[1+\tau_0\frac{d}{dt}\right]\langle S_i(t)\rangle=\langle \tanh(\beta h_i)\rangle \ , \tag{4}$$

where $h_i=\sum_j J_{ij}S_j$ is the exchange field acting on S_i. By a symmetry argument, the right-hand side of Eq. (4) can be expressed as a polynomial containing products of odd numbers of spins. The order of this polynomial p, depends on the local coordination number z. For odd z, p is equal to z and for even z it is equal to $z-1$. In the case of clusters containing not more than seven spins the highest z available is 6 and then

$$\tanh(\beta h_i)=\sum_j{}'\gamma_{ij}S_j+\sum_{\substack{jkl\\ j\neq k\neq l}}\Gamma_{i;jkl}S_jS_kS_l$$

$$+\sum_{jklmr}\tilde{\Gamma}_{i;jklmr}S_jS_kS_lS_mS_r \ . \tag{5}$$

The coefficients γ, Γ, and $\tilde{\Gamma}$ depend on T and the exchange couplings. They can be found by using the representation (5) for all configurations of spins surrounding site i.

Clearly, Eq. (4) couples $\langle S_i \rangle$ to higher-order odd-spin correlations for which analogous equations of motion can be written. For a cluster of n spins there can be all together 2^{n-1} odd-spin correlations which are all coupled within themselves in a linear fashion. Similarly, the $2^{n-1}-1$ even-spin correlations are also coupled linearly within themselves. These, however, would not affect the decay of a magnetization.

As explained in more detail in CL and BCM, the relaxation times τ_μ are equal to $-1/\lambda_\mu$, where λ_μ are the eigenvalues of the equations of motion for the correlations. There are thus both odd- and even-spin relaxation times. The longest relaxation time is always "odd." The "even" times approach the remaining odd times at low T.

We have studied all of the 137 clusters with $n\leq 7$ at various temperatures. Figure 9 shows a distribution of the odd relaxation times at $T=0.2$. Each cluster here is considered on an equal footing, regardless of how probable it may be. The figure shows cumulative distributions for clusters corresponding to a specified number of spins. The immediate observation is that the spectrum is triply partitioned and this property does not depend on n. This reflects—through Eq. (1)—the existence of only three possible energy barriers in the clusters. One can easily

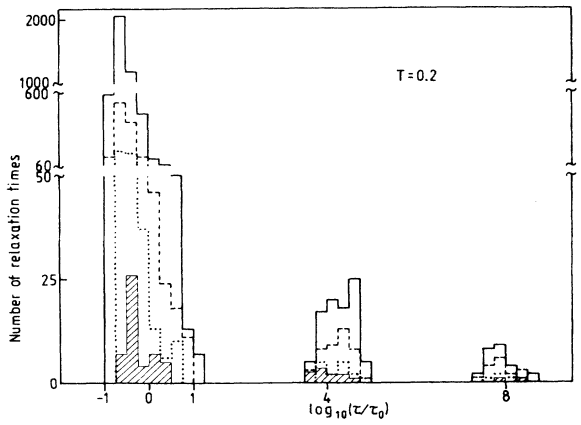

FIG. 9. Distribution of relaxation times at $T=0.2$ (in units of $|J|/k_B$) on the logarithmic scale. The solid line shows numbers of relaxation times found in the $n=7$ clusters, the dashed line in the six-spin clusters, the dotted line in the five-spin clusters, and finally the shaded region corresponds to $n\leq 4$. Each cluster comes with a weight of 1 here. Note that the scale on the vertical axis is broken.

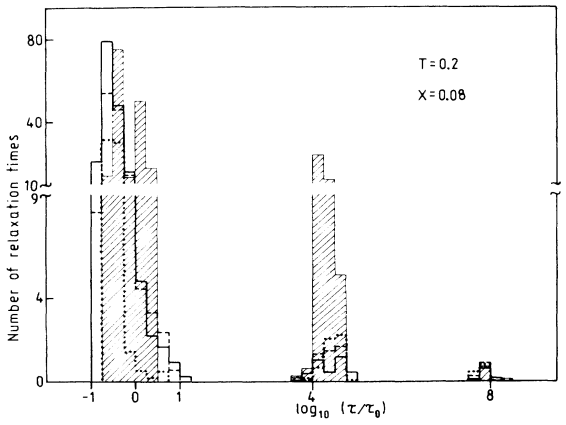

FIG. 10. Same as in Fig. 9, except that each cluster comes with a weight as found at the concentration $x=0.08$.

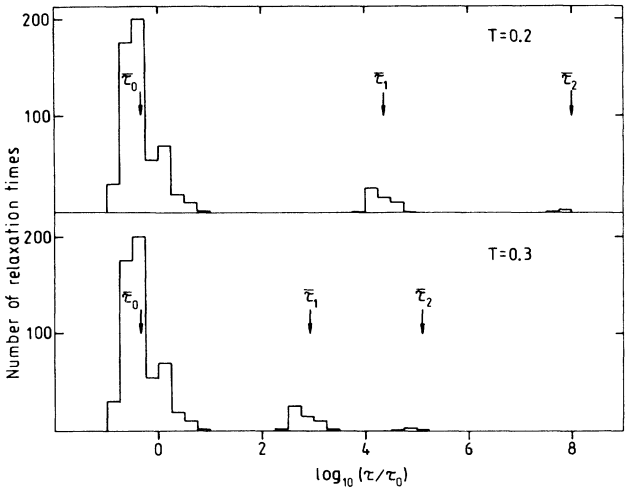

FIG. 11. Distribution of relaxation times for $x=0.08$. The top panel corresponds to $T=0.2$ (in units of $|J|/k_B$), the lower to $T=0.3$. The arrows indicate positions of average relaxation time within each region.

demonstrate that these are equal to 0, $2|J|$, and $4|J|$. The degeneracy in the barriers is due to identical exchange couplings adopted. The prefactors τ_0' of the Arrhenius law differ somewhat between clusters, giving rise to the finite widths in the distribution of the relaxation times.

The short relaxation times, of the order of τ_0, are most ubiquitous. The longest times, of the order of $\tau_0 \exp(4|J|/kT)$, are the rarest. These conclusions are not altered if the statistical weights are attached to the clusters. This is demonstrated in Fig. 10, where the characteristic probabilities for $x=0.08$ are taken into account. The low-n clusters fill most of the "intensity" in the spectrum. Even though the larger-n clusters are more likely to possess more than one long relaxation time than the smaller clusters, their combined weight is not enough to dominate the spectrum.

The combined spectrum, across all $n \leq 7$, is shown in Fig. 11, again at $x=0.08$. The separation between the three regions of the relaxation times shrinks with T. At $T=0.4$ the peaks start to overlap and then they merge into the region of a rapid relaxation. The various relaxation mechanisms separate only at very low T.

Now, how many diverging relaxation times a single cluster can produce? Our studies have brought us to a conclusion that the rules specified in BCM and CŁ need a generalization to cases in which degeneracy in the energy eigenstates is possible. The proper rule is as follows:

The number of the diverging relaxation times in the odd part of the spectrum is equal to the number of nontrivial ordinary energy minima *plus* the number of nontrivial extended energy minima.

In this rule a k-fold extended minimum is meant to contribute only one diverging time, no matter what the value of k. Thus a cluster of kind 2/0 yields two long relaxation times, but a cluster 0/2 yields only one such time. On the other hand, a cluster corresponding to the symbol $0/2+2$ contributes two long times since the two "basins" are not connected. The cluster of Fig. 5 gives rise to two diverging relaxation times and both of them correspond to the same barrier, $\varepsilon=2|J|$. The two times appear different because the τ_0' factors are not the same.

Our rule specifically excludes the totally frustrated states since such states offer no hindrance to up-down global rotations. Thus the 0/0 clusters participate only in rapid processes. On the other hand, if a system is found in an extended minimum, it can "float" in restricted directions, but no full relaxation is possible without making a coupling to a heat bath.

The number of clusters that produce multiple long relaxation times grows with n. For $n=4$, 5, 6, and 7 there are 1, 2, 11, and 36 such clusters, respectively. Out of about 200 different relaxation times identified in the 137 clusters with $n \leq 7$, there were 130 which were due to ordinary energy minima. The role of extended minima in producing a long relaxation, relative to that of the ordinary minima, seems to increase with n. A static magnetic field invalidates the rule linking minima to the relaxation times, similar to what has been found in CŁ.

VI. DYNAMIC SUSCEPTIBILITY

Finding χ' and χ'' requires knowledge of the eigenvectors of the matrix representing the equations of motion. Both odd and even parts are needed since the oscillatory magnetic field couples the two submatrices to each other. The procedure of calculating the dynamic susceptibility of a cluster has been fully described in CŁ.

Consider first the T dependence of χ'. Figure 12 shows the real part of the dynamic susceptibility for two different frequencies and at $x=0.08$. It also shows how each of the three major types of clusters contributes to the net susceptibility. Generally, χ' is expected to follow the equilibrium susceptibility at higher temperatures when the relaxation processes are fast. Upon lowering T, fluctua-

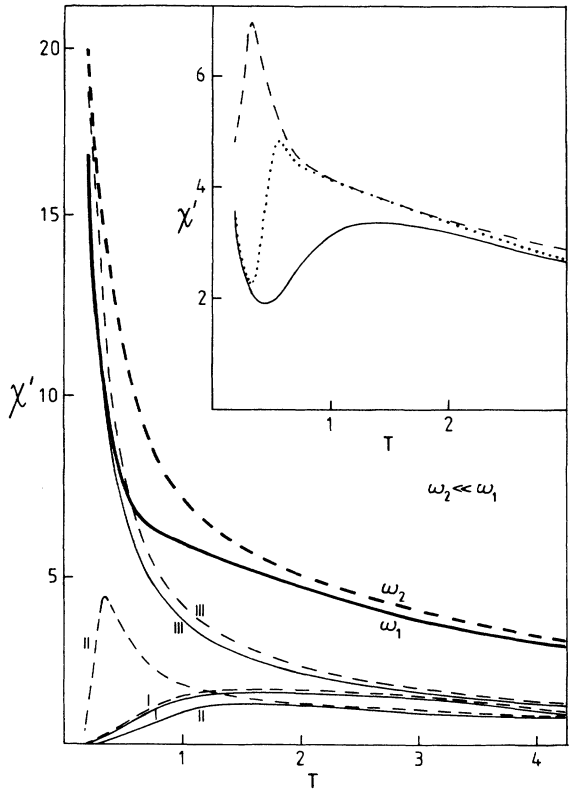

FIG. 12. The real part of the dynamical susceptibility vs T at $x=0.08$ and for two frequencies. The bold solid lines show a net χ', whereas the thin solid lines correspond to contributions of the three major types of clusters as indicated. The solid lines refer to $\omega=\omega_1=0.3/\tau_0$, the dashed to $\omega=\omega_2=8\times10^{-5}/\tau_0$. Inset: a net χ' without the contribution of the single spins. The solid and dashed lines correspond to ω as before. The dotted line corresponds to $\omega_3=1\times10^{-2}/\tau_0$.

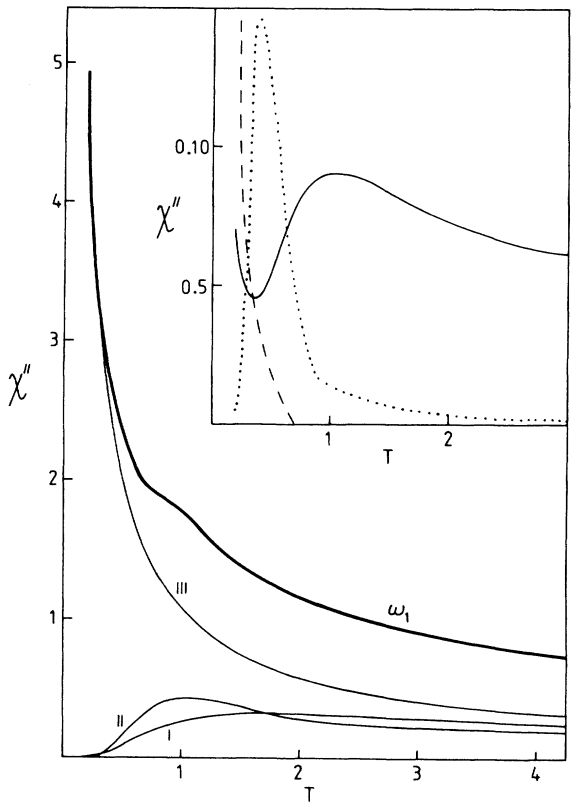

FIG. 13. Same as in Fig. 12, but for χ''. The main figure yields data only for $\omega=\omega_1$.

tions may appear freezed out if the period of oscillations is shorter than the relevant relaxation times. In this case χ' must fall away from χ_{eq} and eventually vanish at $T=0$. The "cusp" moves towards lower T upon decreasing ω.

This pattern is indeed followed by clusters of types I and II. In the former case χ_{eq} tends to zero anyway, so there is no much more fluctuations to freeze out. In the latter case χ_{eq} diverges and χ' behaves in a standard expected way as described, e.g., in CL. The clusters of type III are very different. Their static susceptibility diverges and so does χ'. The reason is that if at least one of the ground states is extended the system will always fluctuate. Some of the spins in the ground states may flip in an immediate response to an ac field. The system behaves as though it consisted merely of unconnected spins. In fact, the single spins constitute the bulk of this kind of cluster. The inset of Fig. 12 shows χ' without the contribution due to the single spins. Now the clusters of type III dominate only at very low temperatures. At intermediate temperatures a kinklike shape is possible. This is similar to an effect found in the ensembles of rings.[8] There the single spins do not appear.

Figure 13 shows χ'' versus T. The temperature dependences of the three types of clusters are as in the case of χ'. We should point out at this stage that at very low temperatures even a tiny scatter in the exchange couplings due to local deformations will effectively transform an extended minimum into an ordinary one. Thus the clusters of type III will yield a $\chi''(\omega)$ which will eventually vanish at $T=0$.

We now examine the ω dependence of the susceptibility. We pick $T=0.2$ and 0.3 to have the time scales sufficiently separated and we take $x=0.08$. Figure 14 demonstrates that the existence of the gaps in the spectrum of relaxation times results in plateaus, when χ' is plotted against $\log\omega$. The rises in χ' upon decreasing ω occur in the vicinities of the inverses of the relaxation times involved. Since there are essentially three groups of such times, we get three inclined and three flat parts in χ'. At $T=0.2$, however, the third plateau is at frequencies still lower than shown in the figure. If there were no gaps in the spectrum, the flat regions would shrink to zero.

Figure 15 plots χ'' versus $\log\omega$. We see that χ'' consists of essentially three maxima located at frequencies within the regions of rises in χ'. We find that the shape of χ'' mirrors the shape of the spectrum of the relaxation times. The peaks in χ'' begin to merge with each other at

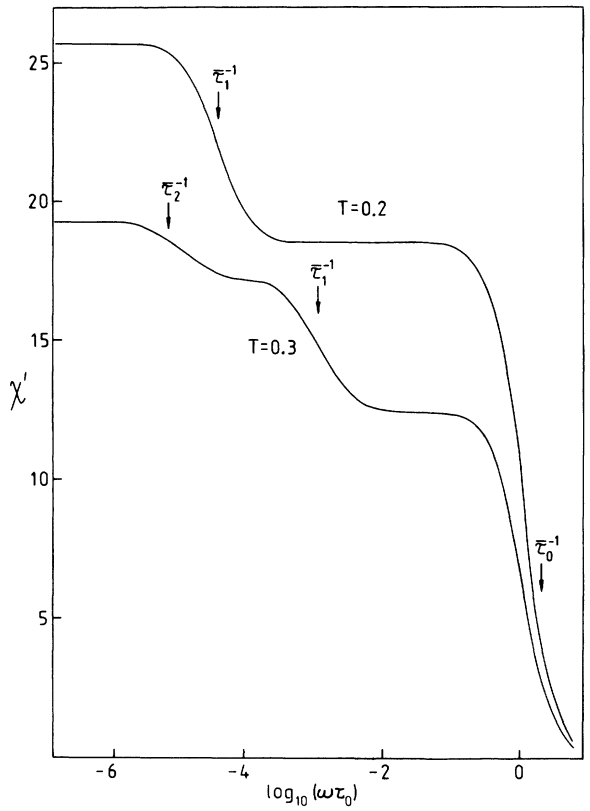

FIG. 14. $\chi'(\omega)$ at $x=0.08$. The times $\bar{\tau}_i$, in units of τ_0, are as in Fig. 11. The upper curve is for $T=0.2$ and the lower for $T=0.3$ (in units of $|J|/k_B$).

$T=0.4$.

The imaginary part of the susceptibility appears to satisfy an approximate relation

$$\chi''(\omega)\cong -b\frac{\partial\chi'(\omega)}{\partial \ln\omega} \tag{6}$$

with $b=1$. The right-hand side of Eq. (6) is also shown in Fig. 15. Lundgren *et al.*[3] derive a b of $\pi/2$. This conclusion, however, depends on the assumption of log-uniform relaxation times.

We close by showing the so-called Argand, or the Cole-Cole plots,[27] in which it is customary to present the dynamical susceptibility. These are given in Fig. 16. For $T=0.3$ we have three semicircles corresponding to the three-piece structure of the susceptibilities. Upon increasing T to 0.4, the longest relaxation times begin to merge and so do the smaller semicircles. On the other hand, decreasing T to 0.2 expands the semicircles. The smallest semicircle here, corresponding to the longest processes, is outside of the figure. We did not calculate it for technical reasons. Note that in the case of rings with Gaussian couplings, the Argand plots are elliptic and not structured.[8]

VII. CONCLUDING REMARKS

The multipeaked χ'' as plotted against $\log\omega$ has been already found in CŁ for a single six-spin cluster with "Gaussian" couplings. This structure also results from a time-scale separation at low T. The novelty of the current study is a prediction of a structured χ'' and χ' for an ensemble of 137 different clusters mimicking magnetic properties of, say, $Cd_{1-x}Mn_xTe$ and $Hg_{1-x}Mn_xTe$.

It seems worthwhile to attempt to detect these features experimentally. Figure 14 tends to suggest a MHz range. Getting to too low temperatures may involve the dipolar

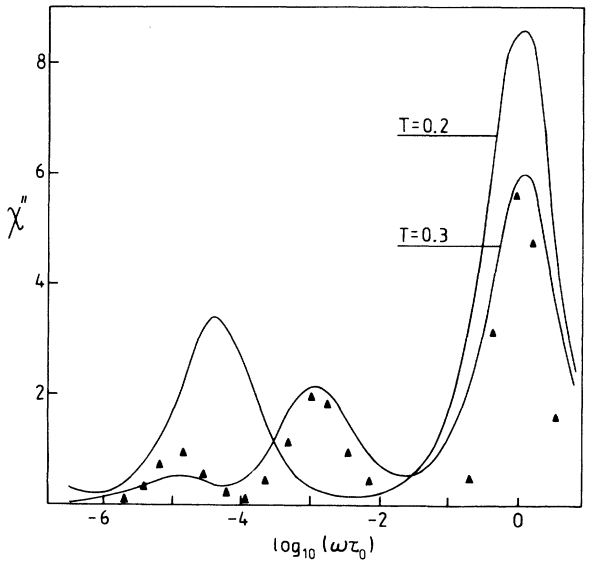

FIG. 15. Same as in Fig. 14, but for $\chi''(\omega)$. The triangles indicate $-b[\partial\chi'(\omega)/\partial\ln\omega]$ with $b=1$ for $T=0.3$ (in units of $|J|/k_B$).

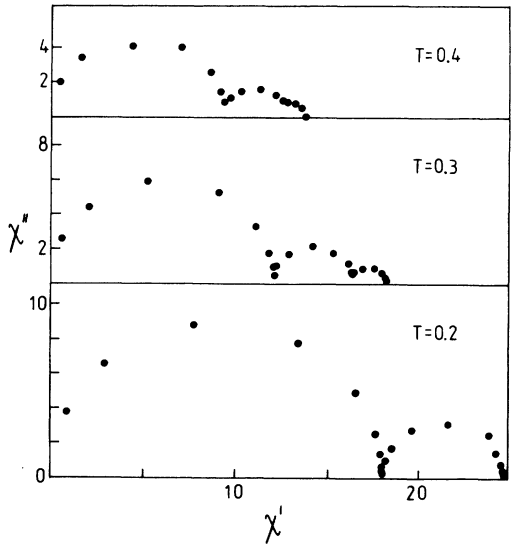

FIG. 16. The Argand plots of χ'' vs χ' for three temperatures as indicated. The data points correspond to $x=0.08$. The smaller the radius of a semicircle, the longer the time scales involved are.

interactions and is thus not recommended. However, at $T=0.4$ and 0.5 there are still two (and not three) time scales which are separated well enough to produce plateaued χ'. Even a negative result would be interesting. An absence of the structures would probably point to relaxation processes which are dominated by the transverse components of the exchange couplings. At the same time the critical properties would be dominated by Ising-like couplings arising via some anisotropies.

In a recent paper Rigaux *et al.*[28] report on measurements of the dynamical susceptibility of $Hg_{1-x}Mn_xTe$ at $x=0.30$. They interpret the data in terms of a wide distribution of relaxation times and get $b \cong \pi/2$ [see Eq. (6)] as in metallic spin glasses. Certainly at this composition the cluster picture should not be applied and the time scales are much longer. The physics of discrete energy barriers should still be valid though. It would be interesting to find out whether there is a frequency range in which the dynamic susceptibility looks structured in this system.

ACKNOWLEDGMENTS

The idea of this project was discussed with the late J. Mycielski. Discussions with T. Dietl were of great help, as were comments by I. Białynicki-Birula. One of us (M.C.) acknowledges the support of the Polish Ministry of Science and Higher Education, Project No. MRI7. Another of us (M.Z.C.) performed part of the calculations at Rutgers University, and was supported by National Science Foundation Grant No. DMR-83-19941.

[1]See, e.g., R. V. Chamberlin, G. Mozurkevich, and R. Orbach, Phys. Rev. Lett. **52**, 867 (1984).
[2]F. Mezei and A. P. Murani, J. Magn. Magn. Mater. **14**, 211 (1980).
[3]L. Lundgren, P. Svedlindh, and O. Beckman, J. Magn. Magn. Mater. **25**, 33 (1981).
[4]L. Lundgren, P. Svedlindh, and O. Beckman, J. Phys. F **12**, 2663 (1982); Phys. Rev. B **26**, 3990 (1982).
[5]L. Lundgren, P. Svedlindh, P. Nordblad, and O. Beckman, Phys. Rev. Lett. **51**, 911 (1983).
[6]W. Kinzel, Phys. Rev. B **26**, 6303 (1982).
[7]J. R. Banavar, M. Cieplak, and M. Muthukumar, J. Phys. C **18**, L157 (1985).
[8]J. D. Reger and K. Binder, Z. Phys. B **60**, 137 (1985).
[9]M. Cieplak and J. Łusakowski, J. Phys. C **19**, 5253 (1986).
[10]R. J. Glauber, J. Math. Phys. **4**, 294 (1963).
[11]G. Eiselt, J. Kötzler, H. Maletta, D. Stauffer, and K. Binder, Phys. Rev. B **19**, 2664 (1979).
[12]J. Mycielski, in *Proceedings of the Sixth International Conference on Ternary and Multiternary Compounds,* edited by B. R. Pamplin *et al.* (Pergamon, Oxford, 1985).
[13]R. R. Gałązka, J. Cryst. Growth **72**, 364 (1985).
[14]R. R. Gałązka, S. Nagata, and P. H. Keesom, Phys. Rev. B **22**, 3344 (1980).
[15]S. Nagata, R. R. Gałązka, D. P. Mullin, H. Akbarzadeh, G. D. Khattak, J. K. Furdyna, and P. H. Keesom, Phys. Rev. B **22**, 3331 (1980).
[16]J. Spałek, A. Lewicki, Z. Tarnawski, J. K. Furdyna, R. R. Gałązka, and Z. Obuszko, Phys. Rev. B **33**, 3407 (1986).
[17]G. S. Grest and E. F. Gabl, Phys. Rev. Lett. **43**, 1182 (1979).
[18]N. B. Brandt, V. V. Moshchalkov, A. D. Orlov, L. Skrbek, I. M. Tsidil'kovskii, and S. M. Chudinov, Zh. Eksp. Teor. Fiz. **84**, 1050 (1983) [Sov. Phys.—JETP **57**, 614 (1983)].
[19]M. A. Novak, O. G. Symko, D. J. Zheng, and S. Oseroff, Phys. Rev. B **33**, 6391 (1986).
[20]A. Twardowski, C. J. M. Dennissen, W. J. M. de Jonge, A. T. A. M. de Waele, M. Demianiuk, and R. Triboulet, Solid State Commun. **59**, 199 (1986).
[21]J. Ferré, M. Ayadi, and A. Mauger, in *Heidelberg Colloquium on Glassy Dynamics and Optimization,* edited by L. Van Hemmen and I. Morgenstern (Springer, Heidelberg, 1986).
[22]F. Keffer, in *Handbuch der Physik,* edited by S. Flügge (Springer, Berlin, 1966), Vol. 18B.
[23]K. Binder and A. P. Young, Rev. Mod. Phys. **58**, 801 (1986).
[24]J. R. Banavar and M. Cieplak, Phys. Rev. Lett. **48**, 832 (1982).
[25]W. L. McMillan, Phys. Rev. B **31**, 342 (1985).
[26]M. Cieplak, G. Ismail, and J. Łusakowski J. Phys. C **20**, 1301 (1987).
[27]See, e.g., R. M. Hill and A. K. Jonscher, Contemp. Phys. **24**, 75 (1983).
[28]C. Rigaux, A. Mycielski, G. Barilero, and M. Menaut, Phys. Rev. B **34**, 3313 (1986).